Assessment of forces in intradermal injection devices : hydrodynamic versus human factors

Assessment of forces in intradermal injection devices: hydrodynamic versus human factors

Running head: *Forces in ID injections: hydrodynamic vs human factors*

Stijn Verwulgen[1,2,*], Koen Beyers[2,6], Timothi Van Mulder[2,3,4], Thomas Peeters[1], Steven Truijen[5], Francis Dams[1], Vanessa Vankerckhoven[2,4]

Corresponding author:

Stijn Verwulgen

[1]Department of Product Development, Faculty of Design Sciences, University of Antwerp, Antwerp, Belgium

[2]Novosanis, Wijnegem, Belgium

[3] Department of Nursing and Midwifery, University of Antwerp, Wilrijk, Belgium

[4] Vaccine & Infectious Disease Institute, University of Antwerp, Wilrijk, Belgium

[5] Department Rehabilitation Sciences and Physiotherapy, University of Antwerp, Wilrijk, Belgium

[6] Voxdale, Wijnegem, Belgium

* Corresponding author:

Stijn.verwulgen@uantwerpen.be

Universiteit Antwerpen

Campus Mutsaard

Ambtmanstraat 1, 2000 Antwerpen

Tel: +32 (0)3 205 61 87

Abstract

Purpose. The force that has to be exerted on the plunger for administering a given amount of fluid in a given time, has an important influence on comfort for the subject and usability for the administrator in intradermal drug delivery. The purpose of this study is to model those forces that are subject-independent, by linking needle and syringe geometry to the force required for ejecting a given fluid at a given ejection rate.

Material and methods. We extend the well-known Hagen-Poiseuille formula to predict pressure drop induced by a fluid passing through a cylindrical body. The model investigates the relation between the pressure drop in needles and the theoretic Hagen-Poiseuille prediction and is validated in fifteen needles from 26G up to 33G suited for intradermal drug delivery. We also provide a method to assess forces exerted by operators in real world conditions.

Results. The model is highly linear in each individual needle with R-square values ranging from 75% up to 99.9%. Ten out of fifteen needles exhibit R-square values above 99%. A proof-of-concept for force assessment is provided by logging forces in operators in real life conditions.

Conclusions. The force assessment method and the model can be used to pinpoint needle geometry for intradermal injection devices, tuning comfort for subjects and usability for operators.

Keywords: needle geometry; human factors; flow rate model; injection force; injection devices

Abbreviations: intramuscularly (IM), intradermal (ID), subcutaneously (SC)

Stijn Verwulgen 27/2/18 10:17
Deleted: Needle and syringe geometry directly relates to the

Stijn Verwulgen 27/2/18 10:16
Deleted: that can be administered at a given

Stijn Verwulgen 27/2/18 10:16
Deleted: and with a given force. This

Stijn Verwulgen 27/2/18 09:46
Deleted: both patient

Stijn Verwulgen 27/2/18 10:13
Deleted: establish a method to

Stijn Verwulgen 12/3/18 19:49
Deleted: inking

Stijn Verwulgen 27/2/18 10:09
Deleted: predict the

Stijn Verwulgen 27/2/18 10:12
Deleted: through a given needle in relation to the injection rate

Stijn Verwulgen 27/2/18 10:24
Deleted: that can be used in-vivo

Stijn Verwulgen 27/2/18 10:24
Deleted: .

Stijn Verwulgen 27/2/18 10:25
Deleted: -vivo

Stijn Verwulgen 27/2/18 10:28
Deleted: with optimized

Introduction

The skin represents the largest organ of the human body (1). It consists of three layers: the epidermis, preventing chemicals and micro-organisms entering the body, the dermis playing a role in immunological surveillance, and the hypodermis or sub-cutis that consists mainly of subcutaneous fat providing insulation, restoring trauma and providing energy reserve (2-4). The skin is considered of particular interest for drug delivery due to its unique immunogenic properties and enhanced pharmacokinetics. To date vaccines are mainly administered intramuscularly (IM) with syringe and needle. Literature reports non-inferior immunogenic responses upon intradermal (ID) delivery (5, 6). Comparison of ID and SC administration in type 1 diabetes showed a significant reduction of pain and superior pharmacokinetics. A more than 40% reduction in onset and 24% reduction in offset time could support closed loop therapy based on ID insulin administration (11, 12).

Traditionally, ID injections are mainly achieved via the Mantoux technique: a hypodermic needle is inserted almost parallel, at 5-10 degrees, into the subject's skin to assure that the needle outlet is located in the dermal zone (13). This requires training (14) and it is hard to exclude false-negative injections without bleeding and bruising (15) and is considered to be painful by the patient.

Micro-needle arrays are considered to be a promising technology for ID and trans-dermal drug delivery (16) (17), but are inherently vulnerable to damage caused by insertion forces or forces for drug injection which might run up to 20N or more (18). This can result in a high failure rate in micro needle based drug administration (19). Single needle-syringe systems can reduce failure rate, enhance repeatability of intradermal drug delivery and omit regulatory challenges faced by micro needle arrays. Single needle-syringe systems can facilitate testing and approval as an add-on

Vanessa Vankerckhoven 12/3/18 14:56
Deleted: A dose sparing effect has been addressed when ID delivery is used compared to IM delivery, e.g. an indication of 80% dose sparing in rabies vaccination (7) (8). Elderly vaccination has been demonstrated to be non-inferior for ID compared to IM delivery (5, 6, 9). Insulin was originally administered IM (10) and currently injected subcutaneously (SC).

Stijn Verwulgen 27/2/18 10:39
Deleted: Currently

Stijn Verwulgen 27/2/18 10:32
Deleted: but

Vanessa Vankerckhoven 12/3/18 14:58
Deleted: . Micro-needles

Vanessa Vankerckhoven 12/3/18 14:58
Deleted: . Insertion forces for micro-needle arrays

to existing vaccination technology (20). Adaptors that standardize ID injections offer the advantage to administer various drugs intra-dermally with a single types of standard tuberculin syringe (21, 22). Solutions have been launched in the life-science market to perform ID injections perpendicular to the subject's skin (23) (24) (16, 20), (25) (7). Perpendicular ID injections are promising new solutions since they allow targeting the dermis more precise and standardized, compared to the Mantoux technique, independent of the user's training experience. Also, single needle-syringe perpendicular ID delivery systems may drastically reduce pain compared to IM injections and decrease anxiety due to the short needle length (26). However the design of medical products is a complex process that requires many iterations linking usability factors with design requirements (27). In particular, the optimization of single needle perpendicular ID injections requires optimization for usability for the operator and comfort for the subject.

A major usability factor is the force exerted by the operator to perform the injection (28). Injection rate, duration, volume to be injected and drug viscosity are parameters that directly relate to that force and hence usability of injection devices (29, 30) (31). These parameters also relate to comfort and acceptance of ID devices in subjects. In fact, pain merely relies on infusion rate, rather than on the total injected volume. Virtually painless injected volumes are possible up to 1ml at injection rates of 0.1ml/min (32). On the other hand, subjects do not want to hold an auto injector on place for more than 15 seconds (33). Long injection times might also lead to hazardous situations. Evaluation in patients using an epinephrine auto injector revealed that only 16% of observed injections where performed along the manufacturer's instructions and 76% of failures are due to the patient's inability to hold the device in place to receive the required amount of substance (34).

Stijn Verwulgen 27/2/18 10:40
Deleted: standardize the Mantoux technique or to

Stijn Verwulgen 27/2/18 11:27
Deleted: S

Stijn Verwulgen 27/2/18 10:41
Deleted: The

Vanessa Vankerckhoven 12/3/18 14:59
Deleted: with single needle and perpendicular to the skin, needs

Stijn Verwulgen 27/2/18 11:25
Deleted: Adaptors that standardize ID injections offer the advantage to administer various drugs intra-dermally with a single type of standard tuberculin syringe (21, 22). To exploit all potential advantages of perpendicular ID drug delivery, new adaptors for single needle-syringe systems should be developed (20, 24). Activation and deactivation steps should be optimized for usability (26) in new ID injection devices.

Stijn Verwulgen 27/2/18 10:44
Deleted: nother

Stijn Verwulgen 27/2/18 10:51
Deleted: corresponding forces

Vanessa Vankerckhoven 12/3/18 14:53
Deleted: s

Stijn Verwulgen 27/2/18 11:16
Deleted: greatly influence

Vanessa Vankerckhoven 12/3/18 15:01
Deleted: For example

Vanessa Vankerckhoven 12/3/18 15:01
Deleted: For example, e

Stijn Verwulgen 27/2/18 13:05
Formatted: Font:Times

Stijn Verwulgen 27/2/18 13:05
Formatted: Font:Times

Stijn Verwulgen 27/2/18 13:05
Formatted: Font:Times

There is a current the need to support the design of ID injection devices that are placed perpendicular to the subject's skin, for optimized efficacy, usability and safety. These desired outcomes depend on various parameters and constraints. Firstly, on one hand, the needle should be thin and sharp enough, not to induce pain or inaccuracies when perforating the subject's skin. At the same time, a sharp bevel results in a big outlet, increasing the risk of leakage, either exterior or into the subcutis. Also, the thinner the needle, the more force is to be exerted by operators for administering at the same rate. Secondly, on the other hand, the needle diameter should be big enough, to reduce injection time and forces required for injection. At the same time, a bigger diameter results in a bigger outlet, with similar risk on leakage. Bigger diameters thus result in smaller bevels, enhancing risk for pain when the needle perforates and inserts the subject's skin. Also, pain might increase with higher flow rate and higher viscosity. Thirdly, the length of the needle is bound to similar trade-offs. A fourth type of constraint is induced by new and promising applications in cell therapy. Therapeutic cells are preferably administered ID (35). As these drugs are highly viscous and their efficacy is generally highly sensitive to shear stresses, it is desirable to tune injection forces, ensuring functionality by controlling shear stress and optimizing usability by controlling injection forces.

Probably, the four type of constraints will conflict in the design of new ID injection devices, and therefore be subject to trade-off. These potential conflicting specifications merely depend on geometrical and mechanical specifications of needle and syringe, rather than on the physical and physiological characteristics of subjects' skin. Thus the question arises how to acquire forces require to inject a given substance at a given injection rate in function of needle

Stijn Verwulgen 27/2/18 13:06
Formatted: Line spacing: double

Stijn Verwulgen 27/2/18 13:05
Formatted: Font:Times

Stijn Verwulgen 27/2/18 13:05
Formatted: Font:Times

Stijn Verwulgen 27/2/18 13:05
Formatted: Font:Times

Stijn Verwulgen 27/2/18 13:05
Formatted: Font:Times

Stijn Verwulgen 27/2/18 13:05
Formatted: Font:Times

Stijn Verwulgen 27/2/18 13:05
Formatted: Font:Times

Stijn Verwulgen 27/2/18 13:15
Formatted: Left, Tabs:Not at 0,99 cm + 1,98 cm + 2,96 cm + 3,95 cm + 4,94 cm + 5,93 cm + 6,91 cm + 7,9 cm + 8,89 cm + 9,88 cm + 10,86 cm + 11,85 cm

Stijn Verwulgen 27/2/18 13:05
Formatted: Font:Times

and syringe geometry. These data would allow tuning geometrical and physical needle-syringe parameters in single needle perpendicular ID injection devices, controlling injection rate, injection time and forces in function of intended application, usage and target group.

We provide a model for the injection force of ID injection devices in function of syringe and needle geometry and drug viscosity. We also provide a method to assess actual forces in operators of site. Our model allows controlling injection rate and injection time. This can be used to optimize the usability in the design of new single needle ID injection devices.

Materials and methods

We provide a model for the hydrodynamic force from the fluid going through the syringe and needle. The model is constructed from hydrodynamic considerations and evaluated in 15 commercially available needles suited for intradermal injection, mounted in a commercially available 1ml syringe in a series of controlled experiments.

The friction force can be measured in a power bench or syringe pump. We also present a method to assess the actual total force exerted by operators of site. This is achieved by coupling force resistive sensors to a micro controller platform. Consequently, subject-specific tissue back-pressure and needle insertion force can be assessed by subtracting the hydrodynamic and friction forces from the total force measured.

1. Hydrodynamic model

We construct a model that links needle geometry, flow rate Q, dynamic viscosity μ, specific mass of a liquid ρ and injection force.

Stijn Verwulgen 27/2/18 13:05
Formatted: Font:Times

Stijn Verwulgen 27/2/18 15:10
Formatted: Font:Times

Stijn Verwulgen 27/2/18 15:10
Formatted: Font:Times

Stijn Verwulgen 27/2/18 15:10
Formatted: Font:Times

Stijn Verwulgen 27/2/18 11:08
Deleted: . ... [1]

Stijn Verwulgen 27/2/18 11:01
Deleted: a

Stijn Verwulgen 12/3/18 20:12
Deleted: , together with

Stijn Verwulgen 27/2/18 14:18
Deleted: validate that

Stijn Verwulgen 27/2/18 14:52
Deleted: The total force for ID drug administration consists of four components: 1) the force of the needle penetrating the subject's skin (18), 2) force from tissue back-pressure due to injection of substance (29), 3) force from internal mechanics, e.g. in a classical syringe this only consists of friction between the plunger and housing and 4) hydrodynamic force from the fluid going through the syringe and needle.

Stijn Verwulgen 27/2/18 14:24
Deleted: to assess the hydrodynamic force

Stijn Verwulgen 27/2/18 14:27
Deleted: in-vivo

Both syringe and needle are modeled as cylindrical bodies. Let A be the area of a cross-section of a cylindrical body, P the corresponding perimeter and $D_h = \frac{4A}{P}$ the hydraulic diameter of that cross-section. The velocity of a liquid flowing through that body in function of location is denoted v. The average velocity of the liquid through a cross-section is $\overline{v} = \frac{\iint v \cdot dA}{A}$. Further v_{max} denotes the maximal velocity in a cross-section. The body we consider is vertically oriented in the gravity field with z the vertical coordinate and g the gravity constant. The Reynolds number (dimensionless) of the flow is $Re = \frac{\rho v D_h}{\mu}$. Let d_n be the internal diameter of the needle, l_n the length of needle, v_n be the velocity of the fluid in the needle in function of location and let $\overline{v}_n$ be the average velocity of the fluid in the needle. Concerning the syringe, let $d_s$be the internal diameter of the syringe, which is taken to be equal to the diameter of the plunger in the syringe, and let $\overline{v}_s$ be the average velocity of the plunger in the syringe. The considered fluid is incompressible. The following energy conservation between 2 cross-sections of a flow channel per unit of time holds when there are no transversal pressure gradients in the cross-section:

$$-\Delta p \cdot Q = \rho g \Delta z \cdot Q + \Delta \iint \frac{1}{2}\rho v^2 \, v \cdot \, dA + heat\ losses \quad (1)$$

Mechanical components of this energy conservation law are already given in terms of syringe, needle and fluid characteristics. Heat losses have to be further elaborated. The term on the left side of (1) is the work exerted by the pressure on the liquid flowing in and out of the control volume. On the right hand side of (1), the first term is the increase in potential gravitational energy whereas the second term is the increase of kinetic energy of the liquid flowing through the control volume. The third term is the mechanical energy dissipated into heat. The kinetic energy correction factor α (see e.g. (36)) is defined as

$$\alpha = \frac{\iint \frac{1}{2}\rho v^2 \cdot v \, dA}{\frac{1}{2}\rho \overline{v}^2 Q}$$

With the definition and after dividing by the flow rate Q, equation (1) turns into:

$$-\Delta p = \rho g \Delta z + \Delta \left(\alpha \cdot \frac{1}{2}\rho \overline{v}^2\right) + heat\ losses \quad (2)$$

We further assume that the liquid in the syringe and needle is Newtonian with laminar flow and without wall slips or hampering. For water injections (μ = 1mPas) at 0.85 14µl/s and a 0.26 mm needle, the Reynolds number is 70. ,At 100µl/s and in a 0.13 mm needle the Reynolds number mounts to 1000. For more viscous liquids or drugs in this window of flow rates and needle diameters the Reynolds numbers will even be lower, which is well below 2000 which supports that our model is well in the laminar flow area. For such flow in a long cylindrical body, the velocity profile over a cross-section is parabolic:

Stijn Verwulgen 12/3/18 20:49
Formatted: Font color: Auto

$v = v_{max}\left(1 - \left(\frac{r}{R}\right)^2\right)$. For parabolic velocity profiles in a circular cross-section, we have

$$\alpha = 2 \text{ and } \overline{v} = \frac{1}{2} v_{max}.$$

Starting from equation (2) for the syringe/needle geometry, the pressure drop from the plunger to the exit section of the needle can be rewritten as

$$-\Delta p = \rho g \Delta z + \Delta \left(\rho \overline{v}^2\right) + heat\ losses (3)$$

The gravimetric term is for 100mm height difference of the order of 1000Pa and is neglected. The kinetic term at the syringe plunger ($\overline{v}_s$ limited to 100mm/s) is less than 100Pa and is neglected too. Thus equation (2) becomes

$$|\Delta p| = \rho \overline{v}_n^2 + heat\ losses\ (4).$$

The heat losses or viscous friction losses are composed of 1) the localized entrance losses at the transition from the syringe to the needle and 2) the distributed tube losses

in the needle:

$$\text{heat/friction losses} = \Delta p_{entrance\ loss} + \Delta p_{tube\ loss} \quad (5)$$

Tube losses are given by the Darcy Weisbach equation (37):

$$\Delta p_{tube\ loss} = f \cdot \left(\frac{L}{D_h}\right) \cdot \frac{1}{2}\rho \overline{v}_n^2 \quad (6),$$

with f the Darcy friction factor (dimensionless). For laminar flow of a Newtonian liquid without wall slip it can be shown that $f = \frac{64}{Re}$. Applying this to a needle with circular cross-section, equation (6) turns into the well-known Hagen –Poiseuille equation to model pressure required to eject fluid through a cylindrical needle (33, 38):

$$\Delta p_{tube\ loss} = \frac{128\,\mu L}{\pi d_n^4} Q \quad (7)$$

The entrance losses in (5) are caused by a contracted flow in the entrance zone of the needle. Therefore, the flow requires temporarily a higher kinetic energy than the first term of (4), which is the kinetic energy downstream of this entrance zone. This excess kinetic energy is not completely recovered downstream of the entrance zone and this leads to a pressure drop, which is quadratic with the flowrate and is given by:

$$\Delta p_{entrance\ loss} = k_e \cdot \frac{1}{2}\rho \overline{v}_{n,}^2$$

with k_e the entrance loss coefficient (dimensionless) of the liquid flowing from the syringe into the needle. For circular cross-sections like a syringe needle geometry, these entrance losses are described analytically (39) and for Re > 10 they compare to empirical work (40). Calculated values for k_e range from 0.3 for Re =2000 till 0.5 for Re = 100. Empirical numbers are 2 to 3 times larger (40). As the calculations do not take asymmetric or oscillating solutions into account, k_e is expected to be between 0,5 and 1,5. We set use $k_e = 1$. For circular cross-sections and laminar flow where the kinetic correction factor α equals to 2, the entrance loss amounts to 25% up to 75% of

Stijn Verwulgen 12/3/18 20:43
Deleted: is

the kinetic energy in the flow. The cited values for k_e assume that the flow channel is longer than the distance over which the entrance effect takes place. For Re>50, the ratio between the length L of the entrance effect and the diameter d of the flow channel is (39):

$$L/d = (0.05456\mathrm{Re} - 0.5640 + 0.8476\exp(-0.05869\mathrm{Re}))$$

This shows that the entrance effect is expected to be in the order of 5 to 50 diameters for respectively Re= 100 and Re = 1000, which is well below the length of the needles under study in this article.

The entrance losses in (5) is given by:

$$\Delta p_{entrance\ loss} = k_e \cdot \frac{1}{2}\rho\overline{v}_n^2 \quad (8),$$

with k_e the entrance loss coefficient (dimensionless) of the liquid flowing from the syringe into the needle. Since we have an incompressible fluid,

$$\overline{v}_s \cdot \frac{\pi d_s^2}{4} = \overline{v}_n \cdot \frac{\pi d_n^2}{4},$$

thus the force F_s on the plunger to overcome the pressure drop (4) is given by:

$$F_s = \frac{8\,\pi d_s^4 \mu L}{d_n^4}\overline{v}_s + (2 + k_e) \cdot \frac{1}{2}\rho\frac{\pi d_s^6}{4 d_n^4}\overline{v}_s^2 \quad (9).$$

The total force F_{exp} to be exerted on the plunger to eject the liquid from the syringe is composed of friction of the plunger when moving in the syringe, denoted F_{fric}, and force to overcome pressure drop (9):

$$F_{exp} = F_{fric} + \frac{8\,\pi d_s^4 \mu L}{d_n^4}\overline{v}_s + (2 + k_e) \cdot \frac{1}{2}\rho\frac{\pi d_s^6}{4 d_n^4}\overline{v}_s^2 \quad (10)$$

It will be verified experimentally how well the model by formulas (9) and (10) can predict the force on the plunger F_{exp} as a function of plunger velocity $\overline{v}_s$ for commercially available needles suited for intra dermal injections, by controlling for the variables $\overline{v}_s, d_s, d_n, l_n, \rho$ and μ.

Stijn Verwulgen 12/3/18 21:37
Formatted: Font:Italic

Stijn Verwulgen 12/3/18 21:37
Formatted: Font:Italic

Stijn Verwulgen 12/3/18 21:26
Formatted: Font:12 pt, English (UK)

Stijn Verwulgen 12/3/18 21:03
Formatted: English (US)

2. Controlled experiment

A syringe adaptor was developed to administer fluid ID in a standardized way perpendicular to the skin. The adaptor is used in this study to control needle geometry. The adaptor is a particular realization of a platform (41), on which a realm of syringes with different dimensions and working principles can be built with needle dimensions varying between 26 and 34 G and protruding part of the needle, from the foot of the device ranging from 0.8mm up to 4mm, injecting a pre-defined fixed volume between 0.05cc and 0.3cc. The basic configuration consists of a housing with a needle suited for intradermal drug delivery, an activation mechanism and a skin penetration mechanism.

Fifteen commercially available needles (BD, EXEL, HSW and TSK) were selected to cover a variety of inner diameters $d_n$and lengths l_n and implemented in the housing. A regular syringe of 1 ml was used in the housing (HSW Soft-Ject Low Dead Space Luer Lock). The syringe's inner diameter was assessed with a calliper with an accuracy of 0.02 mm. Each total needle length was assessed with the same calliper. Bevel length was assessed by an optical microscope as a tolerance measure for needle length, denoted z in Figure 1, right.

Stijn Verwulgen 27/2/18 15:31
Formatted: Font:Times

Stijn Verwulgen 27/2/18 15:31
Formatted: Font:Times

Stijn Verwulgen 27/2/18 15:31
Deleted: protruding needle length

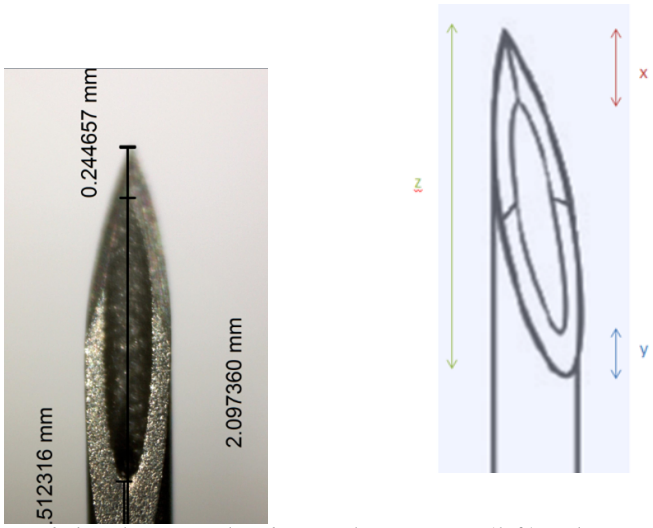

Figure 1: bevel measured with optical microscope (left) and geometrical definition of bevel subtracted from total length in needle length assessment.

Needle diameter $d_s$was assessed through an optical microscope too. Needle types and geometric specifications as provided by manufactures as well as assessed values are displayed in Table I.

The housing with needle and syringe was mounted to a force gauge (Electromatic ESM301) by dedicated designed and 3D printed support parts. Injection speed $\overline{v}_s$was controlled in the power bench. The power bench ensures a constant displacement and thereby returns applied force as a dependent variable. This force has an accuracy of 0.2% according to the manufacturer's specifications, any eventual resulting error is neglected. Friction force of plunger moving in the syringe F_{fric} was assessed by moving the plunger in the syringe in an empty syringe at various speeds in the power bench. The same syringe and plunger was used in all experiments to minimize inter-syringe effects.

Force due to pressure drop through the needle was assessed by subtracting friction force from force assessed while ejecting fluid at the power bench.

For the evaluation of the hydrodynamic model, in total 95 tests were performed, each test with 5 repetitions. In 90 tests, water was used as a liquid. Temperature varied between 15.4°C and 18.5°C. Viscosity was corrected for temperature. Five tests were performed on a water-glycerol mixture with viscosities of respectively 1.1 / 1.5 / 2.1 / 2.9 / 4.3 mPas. In these five tests, a 32G-13mm length needle was used (number 14 in Table I).

All experiments were preformed using a syringe with a diameter d_s = 4.67 mm and velocities $\overline{v}_s$ were set at 50, 125, 175, 200, 250 and 350 mm/min. Measured needle dimensions in Table I were used. In total, 15 types of needles were tested 5 times at these 6 flow rates. Results were analysed in SPSS.

Dynamic viscosity was tuned by water-glycerol mixture. Newtonian behavior was controlled by Rheosense measuring device (Benelux Scientific). In all experiments, temperature was logged to control for eventual viscosity changes. Water-glycerol mixtures were tested at the same temperature (±20°C) as those of the lab during the experiments. The vaccine HBVAXPRO (Sanofi-Pasteur) was tested to compare its behaviour to that of water-glycerol mixtures. All measurements were repeated five times in different shear rates: 2000, 5000, 10000, 15000 and 20000 /s.

3. In vivo force assessment

The effect of the needle gauge on force exerted by operators using the VAX-ID™ syringe adaptor was assessed. The user scenario comprises the following steps: the operator fills the syringe by pulling up liquid from a vial; locks the prefilled syringe without needle in the housing; places the device on the receiver's skin thereby activating the injection mechanism and penetrating the skin; and injects the fluid by a

standard injection mechanism, that is by pushing the plunger, narrowing the syringe's reservoir and thus ejecting the fluid. In a pilot pre-clinical test, only operators are considered. Forces were assessed in 10 voluntary participants. Participants were asked to eject different volumes of demineralized water by pushing on the plunger of the syringe mounted in the housing of the syringe adaptor. No further instructions were given on how to perform the ejection. Fluid was ejected freely in the air without any injection in animal or human tissue, neither artificial substrate. The housing was equipped with a 26G and a 32G needle. A force -resistance sensor FSR-402 from Interlink was mounted on top of the plunger. It has a sensitive diameter of 13 mm and a sensing range from 0.2 N to 20 N with an accuracy of 0.1 N. A connection part was designed and 3D printed for solid mounting the sensor onto the top of the plunger and for distributing force exerted by the operator for stable and repeatable measurements. The set-up was wired to an Arduino microcontroller for read-out by a regular PC.

Results

Needle and syringe parameters

The inner diameter of the syringe was 4.67mm +/- 0.03 mm. Results of all needle measurement are compared with given specifications in Table I.

Table I: Tested needles measured and manufacturer's parameters

Needle #	Brand	Gauge	Spec. diam. (mm)	Spec. length (mm)	Measured Diam. (mm)	Measured length (mm)	Bevel length (mm)
1	BD	26G	0.26	10	0.269	15.651	1.49

Stijn Verwulgen 27/2/18 15:29
Formatted Table

2	BD	26G	0.26	13	0.262	18.857	1.98
3	BD	26G	0.26	16	0.256	22.290	1.90
4	EXEL	27G	0.21	13	0.2160	19.424	1.81
5	HSW FINE	27G	0.21	30	0.212	38.482	1.74
6	HSW FINE	27G	0.21	40	0.208	44.411	1.77
7	HSW FINE	27G	0.21	42	0.213	48.139	1.99
8	HSW FINE	27G	0.21	50	0.210	56.369	1.95
9	EXEL	28G	0.184	20	0.203	27.130	1.39
10	EXEL	30G	0.159	13	0.158 0.157*	22.299	1.39
11	EXEL	30G	0.159	25	0.155	33.952	1.15
12	TSK	31G	0.133	13	0.138	18.635	1.15
13	TSK	32G	0.108	10	0.128	17.923	1.21
14	TSK	32G	0.108	13	0.127 0.130*	18.534	1.05
15	TSK	33G	0.108	13	0.104 0.105*	18.794	0.88

*cross check measurement with electron microscope

The needle length of all evaluated needles was larger than the provided length specifications: needles are prolonged internally in the needle hub, from 5 up to 10 mm.

Specifications were converted from Inch to mm. Most measured inner diameters of the needles correspond to the given specifications, except for the 32G and 28G needles that have larger actual diameters. The 32G-1mm needle has a diameter of 0.127 mm with optical measurement what is just in the specified tolerance limit (0.108 mm +/- 0.019 mm).

Re-assessment with electron microscope yields 0.130mm what falls outside that tolerance limit. For the 28G needle the measured diameter is just within the tolerance limits. In Figure 2, a measurement of needle diameter is displayed for optical and electron microscope. Due to relative long bevels it was impossible to take a sharp image of the entire needle hole, perpendicular to the needle. However detailed partial electron-microscope images (Figure 2, right) indicate that inner wall might have high roughness and might be substantially non-cylindrically shaped.

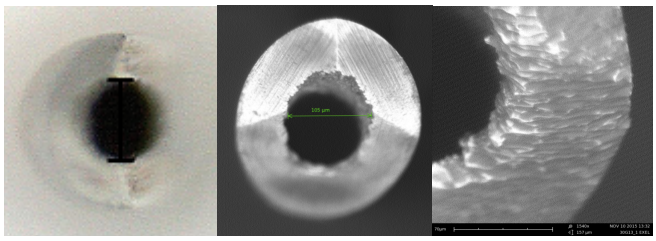

Figure 2: optical assessment of needle diameter (left) and assessment with electron-microscope (middle and right) for a 33G-13 mm length needle

Friction force of plunger moving in the syringe F_{fric} was found to increase with increasing speed, although not linear. Table II shows results of average friction forces under 10 repeated measurements.

Table II: friction force of plunger moving in the syringe at different speeds, controlled by the power bench.

Injection speed (mm/min)	Friction force (SD) in Newton
50	0.561 (0.0722)
125	0.766 (0.0932)
175	0.829 (0.111)
200	0.852 (0.115)
250	0.902 (0.148)
350	1.014 (0.154)

Stijn Verwulgen 27/2/18 15:34
Deleted: -N

Viscosity:

Both water and water-glycerol mixtures demonstrate Newtonian behaviour., i.e. viscosity remains substantially constant when changing the shear rate. HBVAXPRO exhibits non-Newtonian behaviour by shear thinning: the viscosity drops by increasing shear rate. Consequently, the actual hydrodynamic forces could be smaller than the forces provide by our model. Results are displayed in Figure 3.

Stijn Verwulgen 27/2/18 15:54
Formatted: English (UK), Check spelling and grammar

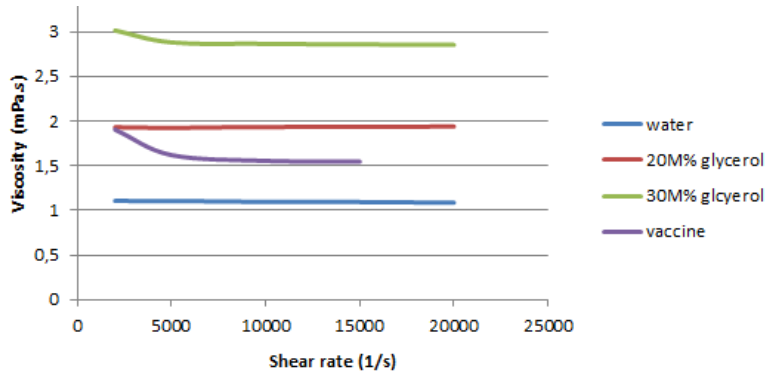

Figure 3: Viscosity in function of shear rate

Evaluation of the proposed hydrodynamic model

The force measurements on the syringe plunger in the test bench are compared to results obtained from formula (10) after controlling for d_s, d_n, $\overline{v}_s$, l_n, ρ and μ. Based on (39) we propose $k_e = 1$ for the entrance loss coefficient. However, since the entrance loss k_e depends on the specific needle's hub geometry, we also evaluate our model for best fit for k_e for any individual needle.

In Figure 4 below, a regression of 90 data points (dotted line) is shown between the measured forces $F_{exp} - F_{fric}$ on the vertical axis and the forces calculated using formula (9) on the horizontal axis.

Stijn Verwulgen 27/2/18 16:18
Formatted: Caption, Centered

Vanessa Vankerckhoven 12/3/18 14:49
Formatted: Font:Italic, English (US)

Stijn Verwulgen 27/2/18 15:55
Deleted: In total 95 tests were performed, each test with 5 repetitions. In 90 tests, water was used as a liquid. Temperature varied between 15.4°C and 18.5°C. Viscosity was corrected for temperature. Five tests were performed on a water-glycerol mixture with viscosities of respectively 1.1 / 1.5 / 2.1 / 2.9 / 4.3 mPas. In these five tests, a 32G-13mm length needle was used (number 14 in T ... [2]

Stijn Verwulgen 27/2/18 16:19
Deleted: these

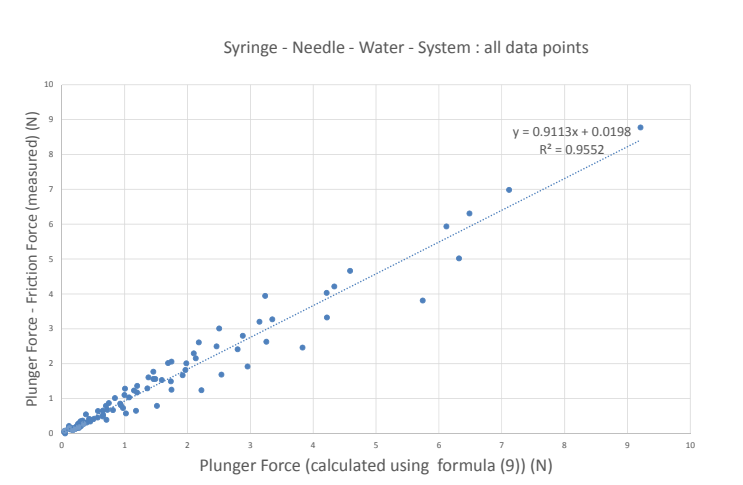

437

438 *Figure 4: Measured forces on the vertical axis versus predicted forces on the*

439 *horizontal axis. Both units at horizontal and vertical axis are Newton (N).*

440 A regression line was calculated yielding

441 $$F_{exp} - F_{fric} = 0.91\, F_s + 0.020N\ ,$$

442 with R^2 =95.5% significant at the 0.001 level and the intercept of 0.020N is in a 95%

443 confidence interval around 0 (t-distribution). The intercept is thus not significantly

444 different from 0 (significance level p = 0.70).

445 The correlation coefficients for the individual needle's regression lines are even much

446 closer to 1 (Figure 5 and Table III).

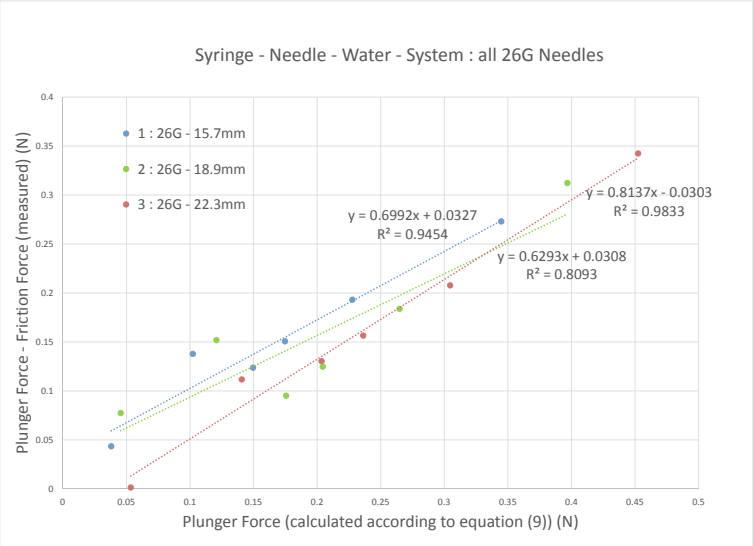
Syringe - Needle - Water - System : all 26G Needles
1 : 26G - 15.7mm
2 : 26G - 18.9mm
3 : 26G - 22.3mm
y = 0.6992x + 0.0327
R² = 0.9454
y = 0.8137x - 0.0303
R² = 0.9833
y = 0.6293x + 0.0308
R² = 0.8093
Plunger Force - Friction Force (measured) (N)
Plunger Force (calculated according to equation (9)) (N)

447

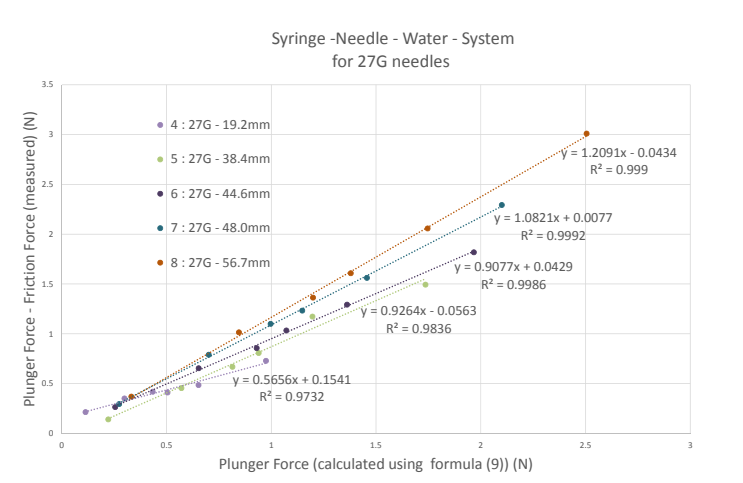
Syringe -Needle - Water - System
for 27G needles
4 : 27G - 19.2mm
5 : 27G - 38.4mm
6 : 27G - 44.6mm
7 : 27G - 48.0mm
8 : 27G - 56.7mm
y = 1.2091x - 0.0434
R² = 0.999
y = 1.0821x + 0.0077
R² = 0.9992
y = 0.9077x + 0.0429
R² = 0.9986
y = 0.9264x - 0.0563
R² = 0.9836
y = 0.5656x + 0.1541
R² = 0.9732
Plunger Force - Friction Force (measured) (N)
Plunger Force (calculated using formula (9)) (N)

448

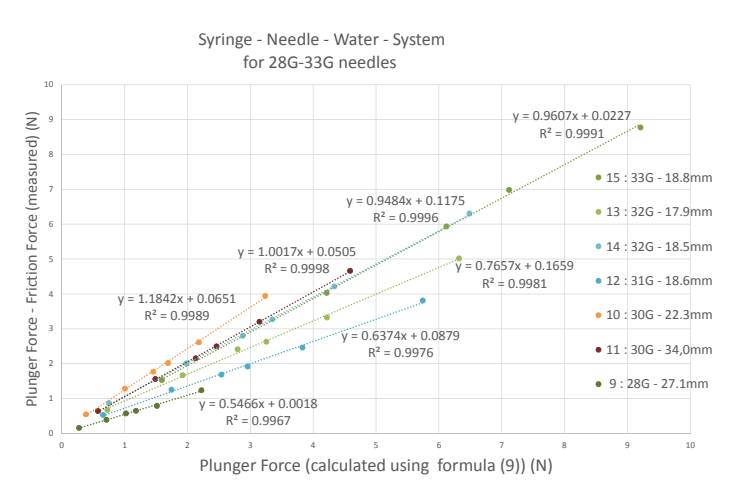

Figure 5: Measured forces Fexp-F_{fric} on the vertical axis versus predicted forces F_s on the horizontal axis for all types of needle. Units on both axis are Newton (N). Numbers 1-15 refer to needle numbers in Table I

Despite correlations of 10 needles are more than 99%, the slopes still vary from 0.55 to 1.21. This suggests that the assessment of individual needle geometry is prone to error, whereas the formula (10) sufficiently models the behaviour for a given needle with accurate geometrical parameters. This is supported by the result that each individual intercept is in a 95% confidence interval around 0. Moreover, corrections on individual diameters to explain slope variation, range between 0.000 and 0.032 mm. In 60% of all evaluated needle, these corrections are within a 10 micron tolerance.

A disagreement between model and measurement can be observed at low plunger force, see Figure 5, especially for 26G and 27G needles. This could possibly be

contributed to enlargement of relative errors on force measurements.

Slope, intercept and correlations for individual needles with $k_e = 1$ are displayed in Table III. The correction on the inner diameter Δd_n to achieve a slope of 1 is displayed in the most right column.

Table III: Regression, slope a, intercept b and R^2 with $F_{exp} - F_{fric} = aF_s + b$, in function of needle geometry, and correction on diameter to provide a slope of 1

Needle #	d_n mm	l_n mm	Slope a	*Intercept b(N)*	R^2	Δd_n mm
1	0.270	15.7	0.70	0.033*	99.8%***	*0.024*
2	0.262	18.9	0.63	0.031*	94.5%***	*0.032*
3	0.256	22.3	0.81	-0.030*	80.9%***	*0.014*
4	0.216	19.2	0.57	0.152	97.9%***	*0.032*
5	0.212	38.4	0.93	-0.056*	97.3%***	*0.004*
6	0.209	44.6	0.91	0.043*	98.4%***	*0.005*
7	0.213	48.0	1.08	0.008*	99.8%***	*-0.004*
8	0.210	56.7	1.21	-0.043*	99.9%***	*-0.010*
9	0.203	27.1	0.55	0.002*	99.9%***	*0.030*
10	0.157	22.3	1.18	0.650*	99.7%***	*-0.007*
11	0.155	34.0	1.00	0.050*	99.9%***	*0.000*
12	0.138	18.6	0.64	0.088*	100.0%***	*0.016*
13	0.13	17.9	0.77	0.166	99.8%***	*0.009*
14	0.130	18.5	0.95	0.118*	99.8%***	*0.002*

15	0.105	18.8	0.96	0.023*	100.0%***	0.001

*** *significant at the 0.001 level* * *within the 95% confidence interval around 0 (t-distribution).*

Finally we display the regression line for the 5 data points on the water glycol mixture in Figure 6 with viscosities varying between 1.1 and 4.3 mPas. This line has a slope of 0.78, an intercept of 0.10N and an R^2= 99.7%, which yields the same conclusions.

Note that for drugs, non-Newtonian behaviour such as shear thinning for HBVAXPRO might influence results, yielding lower actual forces.

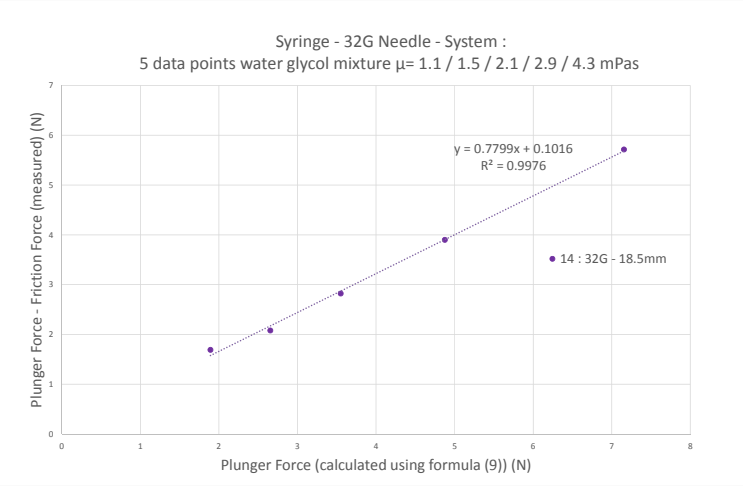

Figure 6: verification of the hydrodynamic model in varying viscosity. Units on both axis are Newton (N)

Force assessment in human operators

Stijn Verwulgen 27/2/18 16:25
Deleted: In vivo f

A total of 10 untrained volunteers were recruited and asked to eject 0.7ml of saline solution with a 1mL SOFT-JECT Luer Lock syringe (Henke Sass Wolf) mounted in the VAX-ID™ adaptor two times: once equipped with a 26G needle and once with a 32G needle. Ejection forces were logged using the FSR sensors coupled to the arduino platform. Results are displayed in Figure 7.

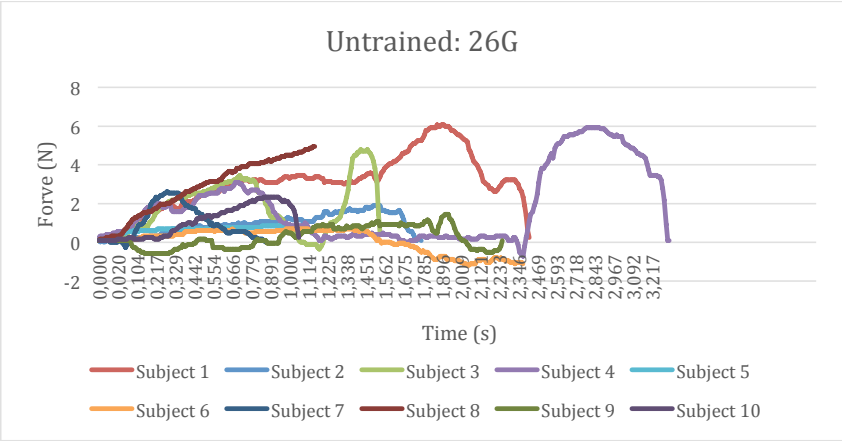

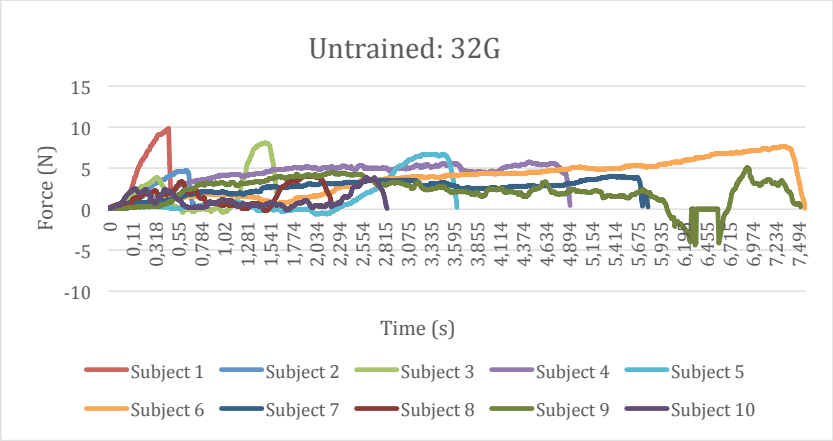

Figure 7: Time logs of forces exerted by non-educated operators with a 26 and 32G hypodermic needle respectively

Stijn Verwulgen 27/2/18 16:26
Deleted: non-educated

Stijn Verwulgen 12/3/18 20:40
Formatted: Centered, Space After: 10 pt, Widow/Orphan control, Adjust space between Latin and Asian text, Adjust space between Asian text and numbers, Tabs:Not at 0,99 cm + 1,98 cm + 2,96 cm + 3,95 cm + 4,94 cm + 5,93 cm + 6,91 cm + 7,9 cm + 8,89 cm + 9,88 cm + 10,86 cm + 11,85 cm

Discussion

Difficult target groups such as children or elderly can benefit from ID drug delivery due to decreased pain, safety and ease of administration. In adults, a needle length of 1mm is most suited for ID injection at the forearm (42). The Mantoux technique can target this depth by stretching the skin to insert a needle with upward tip in the upmost dermal tissue. The Mantoux technique dates from 1910 and to date is still used for e.g. tuberculin and/or HIV infection testing (43) by assessing the bleb visually for antigen reaction. It requires trained medical staff to perform and is limited in needle geometry: relatively large needles of 27 Gauge cause bruising and bleeding but reduce leakage and larger blebs, thereby requiring more training. Relatively small needles of 30 Gauge have more risk of leakage and administering less effective dose (15). Current developments aim to standardize ID injection to enhance reliability with solutions that inject substance perpendicular to the skin.

The total force for such ID drug administration consists of four components: 1) the force of the needle penetrating the subject's skin (18), 2) force from tissue back-pressure due to injection of substance (29), 3) force from internal mechanics, e.g. in a classical syringe this only consists of friction between the plunger and housing and 4) hydrodynamic force from the fluid going through the syringe and needle. By direct acquisition of the third and fourth component and by assessing the actual total force exerted by operators of site, an estimate of the sum of first and second component can be obtained by subtracting the third and fourth component from the actual measurement.

Needle dimensions for ID administration are subject to a trade-off. On one hand, thin needles and blunt beveled needles are preferred for reliably targeting the dermis at 1mm depth without leakage exterior and into to the subcutis. Thin needles can induce

Stijn Verwulgen 12/3/18 20:41
Deleted: A

Stijn Verwulgen 27/2/18 16:47
Deleted: .

Vanessa Vankerckhoven 12/3/18 15:22
Deleted: -

the possibility of self-administration (44). On the other hand, needle diameter should not be too small since higher force required to inject at the same rate might cause discomfort in operators and/or pain in subjects. An upper limit of 30N for injection force was recommended for manual injection into air (30). Also, the formulation of drug and in particular dynamic viscosity relates to bigger needle dimensions (31). Too high shear forces might also influence drug efficacy after administering through microneedles (45).

Tapered microneedles are developed in a trade of between enhanced flow rate and reduced infusion pain (46).

We provide a model for injection forces in cylindrically shaped syringes and needles. Our model extends the well-known Hagen-Poiseuille law (38) and holds with R^2 >99% in 10 out of 15 needles, with a minimum R^2 of 75%. This is remarkable in the light of potential perturbating parameters such as roughness or adhesive forces. We present a method to obtain injection forces in vivo. Preliminary experiments indicate that smaller needles result in bigger injection forces. The method needs to be tuned for robustness and calibrated of-site. Once this tuning is done, we have a method to link user requirements from subjects and operators to syringe and needle geometry, and pinpoint needle dimensions for ID injection devices that are most suited for operator and subject.

This might be achieved in three steps. Firstly, tissue back-pressure during ID injection should be mapped. This can be done by measuring the force during injection and simultaneously tracking the injection rate. The latter can be done by video recording and visually assessing the plunger moving down. Tissue back-pressure is then the difference between measured injection force and forces retrieved from injection rate through our model. Secondly, preferred forces and injection times should be mapped.

Stijn Verwulgen 27/2/18 16:55
Deleted: is

This can be done by inquiring both subjects and operators on what values they consider comfortable. Thirdly, knowledge on tissue back pressure and the present model could be used to select needles that are suitable for ID injections in function of requirements for operator, subjects and intended applications.

Stijn Verwulgen 27/2/18 16:57
Deleted: that yields injection times and forces that are comfortable for both subjects and operators

Conclusions

Needle and syringe geometry directly relates to the amount of fluid that can be administered at a given time and with a given force. The latter two parameters drastically influence comfort of both subject and operator in intradermal drug administration. In the current development of small needles suited for intradermal administration, much effort has gone into the design of the needle's shape.

We have presented a model to predict the force to eject a given fluid through a given needle in function of injection rate. The first part of that force consists of the friction between plunger and syringe. The second part consists of hydrodynamic forces caused by the fluid going through the syringe and needle. The model extends the well-known Hagen-Poiseuille equation used to predict pressure drop induced by a fluid passing through a cylindrical body. The model is highly linear in each individual needle with R-square values ranging from 75% up to 99.9% and 2/3 of these values above 99%. The model was shown to hold for a 1.00ml syringe equipped with needles with inner diameters from 0.10mm up to 0.27mm and needle lengths from 10.0mm up to 50.0 mm and for Newtonian fluids with viscosities from 1.0mPas up to 4.3mPas.

We have additionally presented a proof-of-concept for the system to log injection forces in an in vivo setting. The system and the present model can be used to pinpoint geometrical and physical needle-syringe parameters in single needle perpendicular ID injection devices, controlling injection rate, viscosity, injection time and forces in function of intended application, usage and target group.

Stijn Verwulgen 27/2/18 16:48
Deleted: needle geometry for intradermal injection devices.

Conflict of interest

Authors KB, VVK and SV are co-founders of Novosanis. The other authors report no potential conflict of interest.

Stijn Verwulgen 27/2/18 16:49
Deleted: Thus it can be assured that a given amount of fluid can be administered with forces and times that are comfortable for both subject and operator.

References

1. Slominski A, Wortsman J, Paus R, Elias PM, Tobin DJ, Feingold KR. Skin as an endocrine organ: implications for its function. Drug Discovery Today: Disease Mechanisms. 2008;5(2):e137-e44.
2. Lambert PH, Laurent PE. Intradermal vaccine delivery: will new delivery systems transform vaccine administration? Vaccine. 2008;26(26):3197-208.
3. McGrath J, Uitto J. Anatomy and organization of human skin. Rook's Textbook of Dermatology, Eighth Edition. 2010:1-53.
4. Lai-Cheong JE, McGrath JA. Structure and function of skin, hair and nails. Medicine. 2009;37(5):223-6.
5. Young F, Marra F. A systematic review of intradermal influenza vaccines. Vaccine. 2011;29(48):8788-801.
6. Pileggi C, Lotito F, Bianco A, Nobile CG, Pavia M. Immunogenicity and safety of intradermal influenza vaccine in immunocompromized patients: a meta-analysis of randomized controlled trials. BMC infectious diseases. 2015;15:427.
7. Vescovo P, Rettby N, Ramaniraka N, Liberman J, Hart K, Cachemaille A, et al. Safety, tolerability and efficacy of intradermal rabies immunization with DebioJect™. Vaccine. 2017;35(14):1782-8.
8. Goswami A, Plun-Favreau J, Nicoloyannis N, Sampath G, Siddiqui MN, Zinsou J-A. The real cost of rabies post-exposure treatments. Vaccine. 2005;23(23):2970-6.
9. McElhaney JE, Dutz JP. Better influenza vaccines for older people: what will it take? The Journal of infectious diseases. 2008;198(5):632-4.
10. Rosenfeld L. Insulin: discovery and controversy. . Clinical chemistry, . 2002;48(12):2270-88.
11. Guy R. Transdermal science and technology-an update. Drug Delivery System. Drug Delivery System. 2007;22(4):442-9.
12. Norman JJ, Brown MR, Raviele NA, Prausnitz MR, Felner EI. Faster pharmacokinetics and increased patient acceptance of intradermal insulin delivery using a single hollow microneedle in children and adolescents with type 1 diabetes. Pediatric diabetes. 2013;14(6):459-65.
13. Hickling J, & Jones, R. . Intradermal delivery of vaccines: a review of the literature and the potential for development for use in low-and middle-income countries. . 2009.
14. Tarnow K, King N. Intradermal injections: traditional bevel up versus bevel down. Applied Nursing Research. 2004;17(4):275-82.

15. Flynn PM, Shenep, J. L., Mao, L., Crawford, R., Williams, B. F., & Williams, B. G. Influence of needle gauge in Mantoux skin testing. CHEST Journal. 1994;106(5):1463-5.
16. Kim YC, Jarrahian C, Zehrung D, Mitragotri S, Prausnitz MR. Delivery systems for intradermal vaccination. Current topics in microbiology and immunology. 2012;351:77-112.
17. Larrañeta E, Lutton REM, Woolfson AD, Donnelly RF. Microneedle arrays as transdermal and intradermal drug delivery systems: Materials science, manufacture and commercial development. Materials Science and Engineering: R: Reports. 2016;104:1-32.
18. Lhernould MS, Deleers M, Delchambre A. Hollow polymer microneedles array resistance and insertion tests. International journal of pharmaceutics. 2015;480(1-2):152-7.
19. Van Damme P, Oosterhuis-Kafeja F, Van der Wielen M, Almagor Y, Sharon O, Levin Y. Safety and efficacy of a novel microneedle device for dose sparing intradermal influenza vaccination in healthy adults. Vaccine. 2009;27(3):454-9.
20. Hickling JK, Jones KR, Friede M, Zehrung D, Chen D, Kristensen D. Intradermal delivery of vaccines: potential benefits and current challenges. Bulletin of the World Health Organization. 2011;89(3):221-6.
21. Norman JJ, Gupta J, Patel SR, Park S, Jarrahian C, Zehrung D, et al. Reliability and accuracy of intradermal injection by Mantoux technique, hypodermic needle adapter, and hollow microneedle in pigs. Drug delivery and translational research. 2014;4(2):126-30.
22. Tsals I. Usability evaluation of intradermal adapters (IDA). Vaccine. 2016.
23. Laurent PE, Bonnet S, Alchas P, Regolini P, Mikszta JA, Pettis R, et al. Evaluation of the clinical performance of a new intradermal vaccine administration technique and associated delivery system. Vaccine. 2007;25(52):8833-42.
24. Kis EE, Winter G, Myschik J. Devices for intradermal vaccination. Vaccine. 2012;30(3):523-38.
25. Terumo. Innovating to Create Value through New Perspectives and Synthesis. 2016.
26. Van Mulder TJ, Verwulgen S, Beyers KC, Scheelen L, Elseviers MM, Van Damme P, et al. Assessment of acceptability and usability of new delivery prototype device for intradermal vaccination in healthy subjects. Human vaccines & immunotherapeutics. 2014;10(12):3746-53.
27. Pietzsch JB, Shluzas LA, Paté-Cornell ME, Yock PG, Linehan JH. Stage-gate process for the development of medical devices. Journal of medical devices. 2009;3(2):021004.
28. Cilurzo F, Selmin F, Minghetti P, Adami M, Bertoni E, Lauria S, et al. Injectability evaluation: an open issue. AAPS PharmSciTech. 2011;12(2):604-9.
29. Allmendinger A, Mueller R, Schwarb E, Chipperfield M, Huwyler J, Mahler HC, et al. Measuring tissue back-pressure--in vivo injection forces during subcutaneous injection. Pharmaceutical research. 2015;32(7):2229-40.
30. Burckbuchler V, Mekhloufi G, Giteau AP, Grossiord JL, Huille S, Agnely F. Rheological and syringeability properties of highly concentrated human polyclonal immunoglobulin solutions. European journal of pharmaceutics and biopharmaceutics : official journal of Arbeitsgemeinschaft fur Pharmazeutische Verfahrenstechnik eV. 2010;76(3):351-6.

Koen Beyers 13/3/18 21:22
Formatted: Dutch

31. Adler M. INJECTABLES-Challenges in the Development of Pre-filled Syringes for Biologics from a Formulation Scientist's Point of View. American Pharmaceutical Review. 2012;15(1):96.
32. Gupta J, Park SS, Bondy B, Felner EI, Prausnitz MR. Infusion pressure and pain during microneedle injection into skin of human subjects. Biomaterials. 2011;32(28):6823-31.
33. Fry A. Injecting Highly Viscous Drugs. Pharmaceutical Technology. 2014;38(11).
34. Bonds RS, Asawa A, Ghazi AI. Misuse of medical devices: a persistent problem in self-management of asthma and allergic disease. Annals of Allergy, Asthma & Immunology. 2015;114(1):74-6. e2.
35. Leoni G, Lyness A, Ginty P, Schutte R, Pillai G, Sharma G, et al. Preclinical development of an automated injection device for intradermal delivery of a cell-based therapy. Drug delivery and translational research. 2017;7(5):695-708.
36. Sadri R, Floryan J. Accurate evaluation of the loss coefficient and the entrance length of the inlet region of a channel. Journal of fluids engineering. 2002;124(3):685-93.
37. Brown GO. The history of the Darcy-Weisbach equation for pipe flow resistance. Environmental and Water Resources History2003. p. 34-43.
38. Sutera SP, Skalak R. The history of Poiseuille's law. Annual Review of Fluid Mechanics. 1993;25(1):1-20.
39. Santos RGd, Figueiredo JR. Laminar elliptic flow in the entrance region of tubes. Journal of the Brazilian Society of Mechanical Sciences and Engineering. 2007;29(3):233-9.
40. Idelchik I, Steinberg M, Malyavskaya G, Martynenko O. Handbook of Hydraulic Resistance1994.
41. Simpson TW, Maier JR, Mistree F. Product platform design: method and application. Research in Engineering Design. 2001;13(1):2-22.
42. Van Mulder T, de Koeijer M, Theeten H, Willems D, Van Damme P, Demolder M, et al. High frequency ultrasound to assess skin thickness in healthy adults. Vaccine. 2017;35(14):1810-5.
43. Salgame P, Geadas C, Collins L, Jones-Lopez E, Ellner JJ. Latent tuberculosis infection--Revisiting and revising concepts. Tuberculosis. 2015;95(4):373-84.
44. Yamada S, Yamada Y, Tsukamoto Y, Tabata M, Irie J. A comparison study of patient ratings and safety of 32-and 34-gauge insulin pen needles. Diabetology International. 2016;7(3):259-65.
45. Li M, Tian X, Schreyer DJ, Chen X. Effect of needle geometry on flow rate and cell damage in the dispensing-based biofabrication process. Biotechnology progress. 2011;27(6):1777-84.
46. Martanto W, Baisch SM, Costner EA, Prausnitz MR, Smith MK. Fluid dynamics in conically tapered microneedles. AIChE Journal. 2005;51(6):1599-607.

Koen Beyers 13/3/18 21:22
Formatted: Dutch